Journal of Energy
VOLUME 75 Number 3 | 2026
journal homepage: http://journalofenergy.com/

Geomagnetically Induced Currents and Influence on Power Transformer Saturation

Antonio Gloc, Bruno Jurišić, Božidar Filipović-Grčić

Summary **—The paper studies geomagnetic disturbances and their impact on the electric power system. The resulting geomagnetically induced currents (GIC) have a very low frequency, in the range of 0.01 Hz to 0.5 Hz, and can therefore be considered quasi-direct current. The entry of direct current into a transformer can lead to its saturation, resulting in excessive heating, a significant increase in reactive power consumption, and the generation of even and odd harmonics. Increased reactive power consumption lowers the voltage in the network, while the produced harmonics interfere with the operation or can trigger unintended activation of relay protection systems or disconnection of reactive power compensators. Simulations were conducted using the EMTP software, in which a model of the IEEE 118-bus test system was developed. The impact of geomagnetic electric fields (GEF) of varying intensities and different angles of incidence relative to transmission lines was analyzed. The transformer connection group, protective measures, key results, and conclusions regarding the simulation of nonlinear and frequency-dependent models are also presented.**

Keywords **— EMTP, Geomagnetic electric field, Geomagnetic storms, Geomagnetically induced current.**

I. Geomagnetically Induced Currents

Geomagnetic disturbances (GMD) are driven by plasma (solar wind) from the Sun that reaches the Earth, where it interacts with the Earth's magnetic field. Result of this interaction is a varying magnetic field (measured in nT) on the Earth's surface. Which leads to the induction of a variable electric field (measured in V/km) that is directly related to the changes of the magnetic field and the conductivity of the Earth's crust and upper mantle, where lower conductivity results in stronger electric field for the same magnetic field. Due to variability in the electric field, a current is induced, hereafter referred to as geomagnetically induced current (GIC). The usual cycle of solar activity is approximately 11 years, with peak years shown in Fig. 1. During peak years of solar activity, large quantities of high-energy particles are emitted from the Sun that reach the Earth within two to three days.

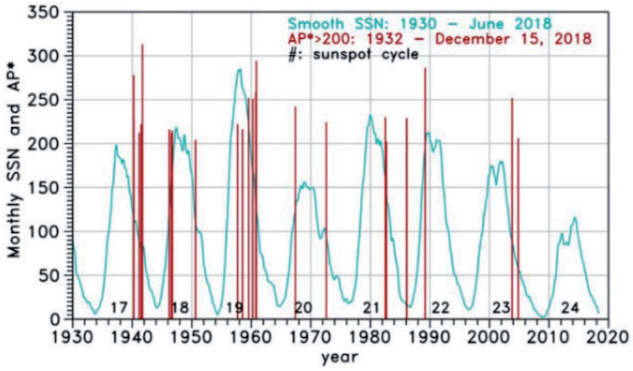

Fig. 1. The sunspot cycle and the occurrence of major geomagnetic storms (SSN1, AP2)

II. Transformer Saturation

When a power transformer is exposed to DC current, a DC flux appears in the magnetic core. The magnitude of this flux depends mainly on the magnitude of the DC current, the number of turns in the windings through which the DC current flows, and the magnetic reluctance of the path for this DC flux. A consequence of the presence of a DC component in the current is that its flux is superimposed on the AC flux during one half-cycle. This asymmetry causes the operating point of the magnetic core to shift toward saturation during one half of the cycle, thereby significantly increasing the peak magnetic flux density in the transformer core. For higher values of DC current, the core presents very high reluctance, which results in a smaller further increase in DC flux density. Accordingly, the magnetizing current becomes a short-duration pulse with a high amplitude. The duration of this pulse ranges from 1/6 to 1/10 of the period of the sinusoidal voltage, as shown in Fig. 2.

(Corresponding author: Antonio Gloc)
Antonio Gloc is with Končar Distribution and Special Transformers Inc., Zagreb, Croatia (email: antonio.gloc@koncar.hr)
Bruno Jurišić is with Končar Electrical Engineering Institute Inc., Zagreb, Croatia , (email: bruno.jurisic@koncar.hr,)
Božidar Filipović-Grčić is with University of Zagreb Faculty of Electrical Engineering and Computing, Zagreb, Croatia
(email: bozidar.filipovic-grcic@fer.hr)

[1] SSN – Smoothed sunspot number.
[2] AP – Instead of calculating only the average of the eight 3-hour "AP" indices centered on each day, the average is computed by including other 24-hour periods that extend from half a day into neighboring days.

Antonio Gloc, Bruno Jurišić, Božidar Filipović-Grčić, Geomagnetically Induced Currents and Influence on Power Transformer Saturation, Journal of Energy, vol. 75 Number 3 (2026), 43–49
https://doi.org/10.37798/2026753768
© 2026 Copyright for this paper by authors. Use permitted under Creative Commons Attribution-NonCommercial (CC BY-NC) 4.0 International License

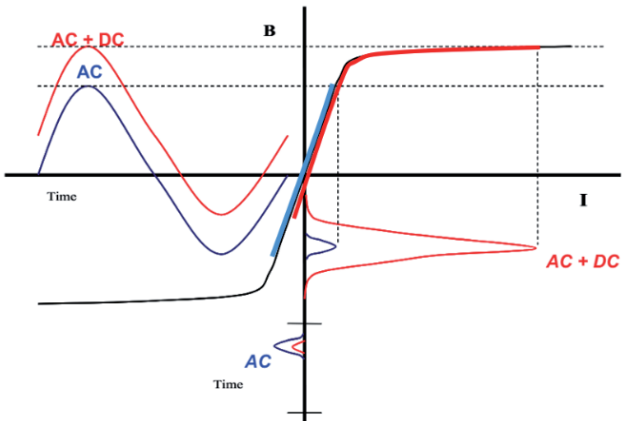

Fig. 2. Transformer core saturation in the presence of superimposed direct current

The increase of DC flux in the core depends on the magnetic reluctance of the DC flux path. Therefore, the increase of DC flux in a three-phase, three-limb transformer would be the smallest among all core designs, because this basic design has an order-of-magnitude higher magnetic reluctance. In this core design, the magnetic flux must traverse a very high-reluctance path, from the upper core yoke to the tank cover, through the tank walls, and then back to the yoke via another high-reluctance path from the bottom of the tank to the lower core yoke.

The five-limb core type has a much lower reluctance because, unlike the three-limb design, it provides a return path for the DC magnetic flux through the core itself, more precisely through the outer core limb. In Fig. 3 (right) DC magnetic flux is illustrated in red, depicting the flux path for a single phase.

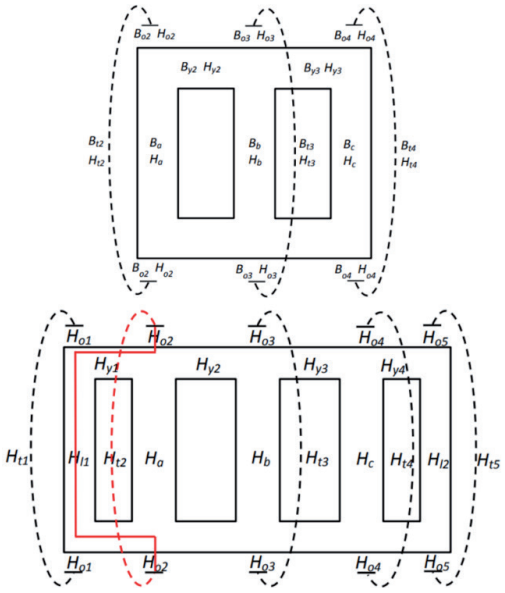

Fig. 3. Schematic diagram of three-limb and five-limb transformers and the paths of DC flux within them

III. Mitigation Of GIC Effects

One of possible mitigation measures includes the installation of a GIC blocking device at the transformer neutral point. By using a capacitor as the blocking device, direct current is completely blocked from flowing through the transformer windings when it is connected between the transformer neutral point and ground. However, because the solid grounding of the neutral point is interrupted, the voltage between the neutral point and ground will increase in the event of a single-phase short circuit. Therefore, the insulation of the transformer neutral point must be reinforced to withstand this condition. In addition, by blocking the entry of direct current into one transformer, the current is redistributed through the ground and may enter and be higher in other transformers within the substation. For this reason, blocking devices would then need to be installed on all transformers within the substation.

Fig. 4 shows a schematic diagram of a DC current blocking device. Through the capacitor, effective grounding is achieved under normal operating conditions (at the power system frequency), while at the same time the passage of DC current is blocked because, at low frequencies, the capacitor represents an open circuit. The parallel thyristor circuit and the low-voltage circuit breaker protect the capacitor from overvoltage that may be caused by high currents flowing through the neutral point in the event of asymmetrical faults. After the breaker operates, the device can be reset using a motor drive, at the same time, the breaker can also be used to switch the device on or off.

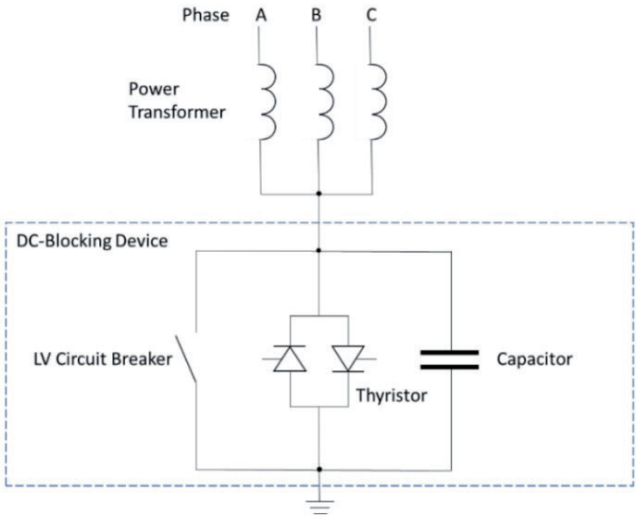

Fig. 4. Schematic diagram of a DC current blocking device

IV. Simulations in EMTP

For the implementation of simulations, the IEEE 118-bus benchmark test network was used in EMTP for GMD. The network consists of 118 nodes with defined geographical coordinates, since the amount of GIC induced in the transmission lines connecting them depends on their location. Fig. 6 depicts a single-line diagram of 118-GMD, which is based on a simplified model of a portion of the American electric power (AEP) system in the U.S. Midwest. The system contains 118 buses at 138 and 345 kV, 177 transmission lines, 91 loads, and 69 synchronous machines (SMs) including SGs (marked by "G") and synchronous condensers (SCs) (marked by "C") for reactive power support. Bus numbers, names, and voltage levels match those of the original case [13].

The geomagnetic electric field (GEF) is modeled as a controllable DC voltage (1) injected into series of each phase of the line. To model the GEF vector shown in Fig. 5, a coordinate system is used where "x" represents north and "y" represents east, with and indicating the electric field in the x and y directions. The angle between the ordinate and the GEF is defined as , and the angle between the ordinate and the orientation of the transmission line in space is defined as . Using those, the angle between the GEF and the transmission line orientation in space, is calculated (2). For

Antonio Gloc, Bruno Jurišić, Božidar Filipović-Grčić, Geomagnetically Induced Currents and Influence on Power Transformer Saturation, Journal of Energy, vol. 75 Number 3 (2026), 43–49
https://doi.org/10.37798/2026753768
© 2026 Copyright for this paper by authors. Use permitted under Creative Commons Attribution-NonCommercial (CC BY-NC) 4.0 International License

the calculations, the line length (3) is also needed, which is obtained from the parameters (4) and (5), representing the distances in the north and east directions, respectively. Those distances are calculated from the geographic coordinates of the nodes that are connected by the line.

$$V_{dc}(t) = l\sqrt{E_x^2 + E_y^2}\cos\big(\theta(t)\big) \quad (1)$$

$$\theta(t) = \theta_L - \theta_{GEF}(t) \quad (2)$$

$$l = \sqrt{l_x^2 + l_y^2} \quad (3)$$

$$l_x = 111.2\big(Lat_i - Lat_j\big) \quad (4)$$

$$l_y = 111.2\big(Long_i - Long_j\big)\sin\Big(90^0 - 0.5\big(Lat_i + Lat_j\big)\Big) \quad (5)$$

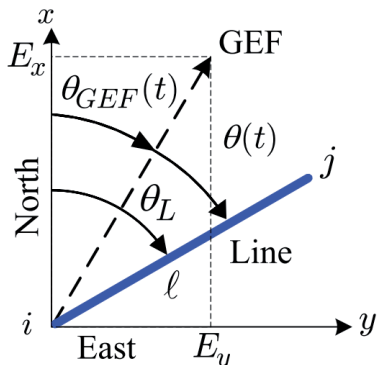

Fig. 5. Defining the coordinate system in GIC analysis

In the model, a GEF with a constant magnitude and angle was used, although under real conditions these parameters vary over time and typically last for 2 to 3 days. The NERC TPL-007 standard defines a reference GMD event, statistically expected once every hundred years, which is used to assess impacts on the power system, Fig. 7. The complete recording of such an event lasts 50 hours, which is an excessively long interval for simulation. However, it has been shown that individual segments, characterized by specific intensity and direction, persist for few minutes with minimal variation.

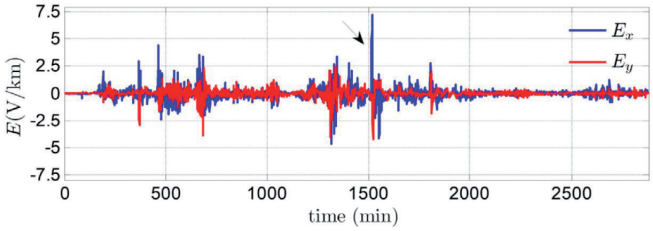

Fig. 7. NERC TPL-007 Reference GMD Event

Therefore, in the model, a series of simulations was conducted using a GEF with a constant magnitude and angle, lasting 400 seconds with a time step of 100 μs, thereby enabling analysis of the impact of the observed GMD on the power system. This approach makes it possible to cover a wide range of potential GMD scenarios while maintaining the complexity and duration of the simulation.

A. Selection of the transmission line model

In the simulations, different transmission line models were used to analyze the impact of the model type on GIC results: the PI model and the FD model. The PI model is generally the most commonly used model and is suitable for medium and long length lines. It provides accurate results and is considered reliable, except during transient events and at high frequencies, where deviations in line impedance can introduce errors in the simulation. The FD model is a frequency dependent model that is more suitable for accurately simulating transients caused by GICs. It addresses line impedance inaccuracies at high frequencies, as shown in Fig. 8. Since the analyzed phenomena involve transformer core saturation and higher-order harmonics, the FD model provides better accuracy in capturing these effects.

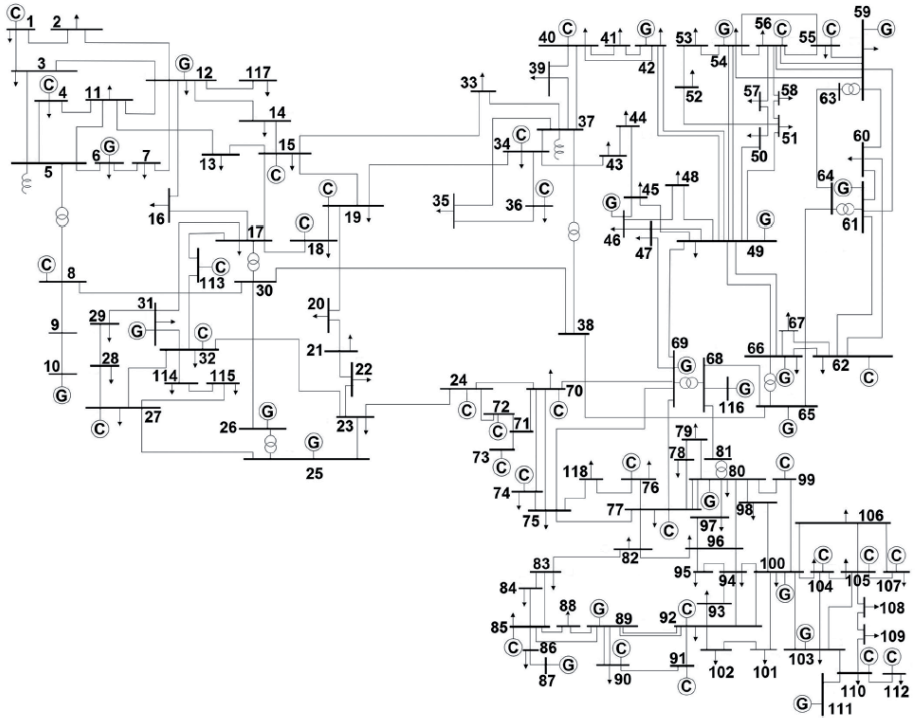

Fig. 6. Single-line diagram of IEEE 118-bus benchmark for GMD

Antonio Gloc, Bruno Jurišić, Božidar Filipović-Grčić, Geomagnetically Induced Currents and Influence on Power Transformer Saturation, Journal of Energy, vol. 75 Number 3 (2026), 43–49
https://doi.org/10.37798/2026753768
© 2026 Copyright for this paper by authors. Use permitted under Creative Commons Attribution-NonCommercial (CC BY-NC) 4.0 International License

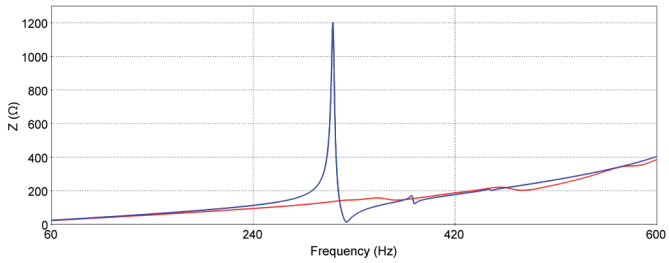

Fig. 8. Comparison of the impedance response in relation to frequency measured at node 10 for the PI and FD transmission line models (PI model – blue, FD model – red)

B. IEEE 118-Bus Network under a 2 V/km GMD

The first simulation was carried out with a GEF amplitude of 2 V/km and an incidence angle on the network of 35°, with the disturbance starting at the 10th second. Effect of disturbance is examined on a step-up single-phase transformer operating in a three-phase configuration, with a rated power of 250 MVA and a rated voltage of 20/345 kV. The transformer is located at node 10 and is connected in the YNd11 vector group. The result of this disturbance is the injection of a negative direct current into the transformer, which shifts the magnetizing current entirely into the negative region of the core's magnetic characteristic Fig. 9.

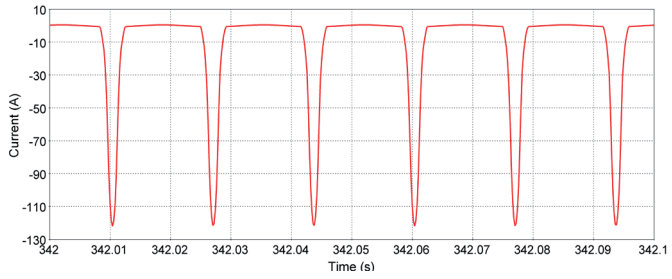

Fig. 9. Magnetizing current of the step-up transformer core at Node 10 during GIC

The amplitude of the magnetizing current increased several times, and the waveform became distorted, indicating the generation of higher harmonics. Fig. 10 shows the presence of both even and odd harmonics in the transformer. The shift in the magnetizing current also impacts reactive power consumption, as the current exceeds the core magnetization knee, leading to a significant increase in reactive power demand Fig. 11.

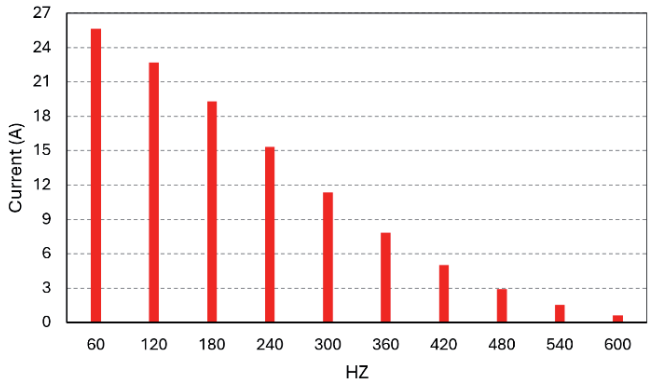

Fig. 10. Harmonic content of the magnetizing current in the power transformer at Node 10

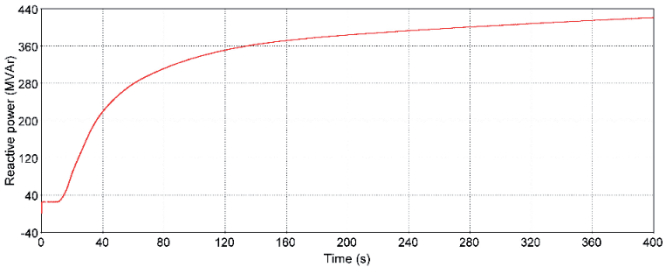

Fig. 11. Total change in reactive power consumption across all connected power transformers under GIC conditions

Change in GEF Direction

In the next simulation, the GEF angle was changed from 35° to 105°, while the amplitude remained unchanged at 2 V/km. Due to the changed angle, voltages of different magnitudes are induced throughout the system, resulting in the injection of currents with different amplitudes into all lines. The magnetizing current is distorted, but its amplitude is smaller in this case because the GEF angle is more favorable Fig. 12. Despite the lower amplitude, both even and odd harmonics are still present, with the same ratio between the higher harmonics and the fundamental harmonic Fig. 13.

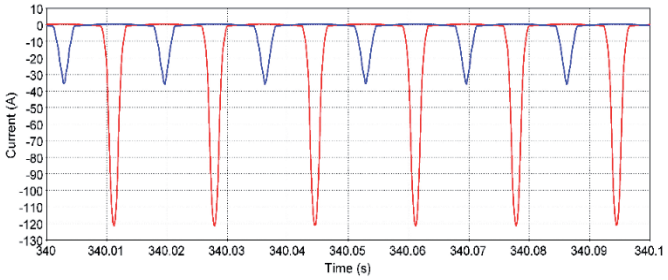

Fig. 12. Magnetizing current of the step-up power transformer core in Node 10 during GIC (GEF 105° – blue line, GEF 35° – red line)

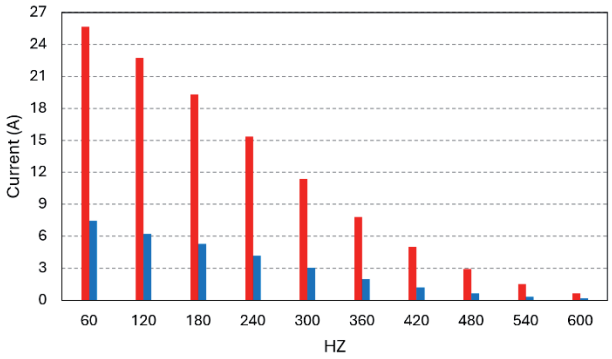

Fig. 13. Harmonic content of the magnetizing current in the step-up power transformer in Node 10 (GEF 105° – blue line, GEF 35° – red line)

Reactive power consumption decreased to 4.96 MVAr, representing a significant reduction compared to the previous simulation value of 16.3 MVAr as show in Fig. 14. Interestingly, the total reactive power consumption of the network did not change substantially, which might have been expected if only results from a single bus were considered. This behavior can be attributed to the large, geographically dispersed network with a high number of transformers. As shown in Fig. 15, the total reactive power consumption reaches 440 MVAr, whereas in the previous simulation at the same instant it was 420.6 MVAr.

Antonio Gloc, Bruno Jurišić, Božidar Filipović-Grčić, Geomagnetically Induced Currents and Influence on Power Transformer Saturation, Journal of Energy, vol. 75 Number 3 (2026), 43–49
https://doi.org/10.37798/2026753768
© 2026 Copyright for this paper by authors. Use permitted under Creative Commons Attribution-NonCommercial (CC BY-NC) 4.0 International License

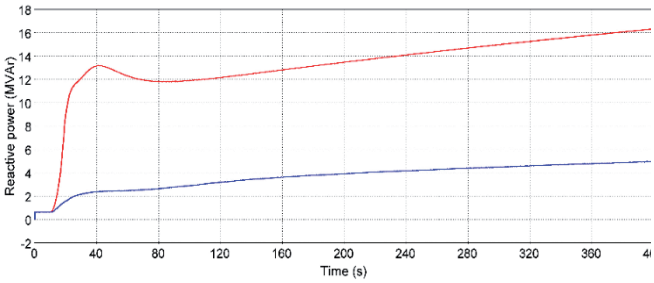

Fig. 14. Change in reactive power consumption of the step-up power transformer in Node 10 (GEF 105° – blue line, GEF 35° – red line)

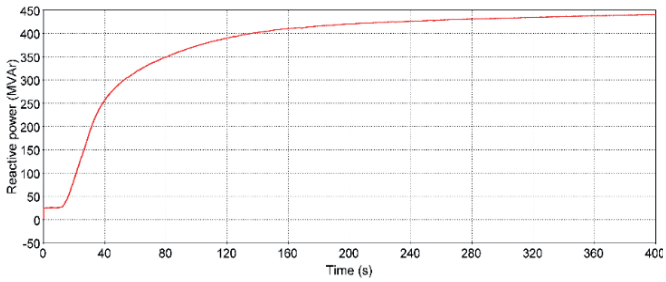

Fig. 15. Total change in reactive power consumption of all power transformers in the system after change in the GEF angle during GIC

D. Transformer star-point grounding via a capacitor

To block or mitigate the impact of GICs in the network, a device for blocking the direct current component was installed in the transformer star point, as described in section III. The simulation focuses on the step-up single-phase transformer at node 42, rated 37.5 MVA and 10.5/138 kV, connected in the YNd11 vector group and operating in a three-phase configuration. In the simulation model, a capacitor with a capacitance of 0.5 μF was connected to the star point of all transformers. Considering the impedance of the capacitor (6), for a current with a frequency of ≈0 Hz, which corresponds to the GIC frequency, the impedance tends toward infinity (7), while for a current at the 60 Hz operating frequency, the impedance (8) is 5.3 kΩ. This means that for DC current, the capacitor behaves as an open circuit, whereas for AC current, it acts as a resistance through which current can still flow (effectively grounding the star point at the operating frequency).

$$X_c = \frac{1}{2 * \pi * f[Hz] * C[F]} \tag{6}$$

$$X_c = \frac{1}{2 * \pi * 0.01[Hz] * 0.5 * 10^{-6}[F]} = 31.83\ M\Omega \tag{7}$$

$$X_c = \frac{1}{2 * \pi * 60[Hz] * 0.5 * 10^{-6}[F]} = 5.31\ k\Omega \tag{8}$$

This solution also has its drawbacks, such as an increase in voltage between the neutral point and ground during a single-phase short circuit, and the diversion of DC current through other nearby transformers that do not have a capacitor installed at the neutral point. Since short-circuit events are not simulated in the model, the blocking device was modeled in the simulations only as a capacitor. Real devices used for DC current blocking also include, in parallel with the capacitor, a low-voltage switch and a thyristor circuit, which are used to protect the insulation of the star point and capacitor from overvoltage during asymmetrical short circuit.

Fig. 16 shows the distorted magnetizing current of the observed transformer during a GIC event prior to the installation of a neutral-point capacitor. With the capacitor installed, the waveform remains largely unchanged, both before and during the GIC, with a negligible amplitude difference of approximately 1 mA, as shown in Fig. 17 and Fig. 18. Harmonic analysis highlights the presence of high-order harmonics before capacitor installation Fig. 19, whereas after installation Fig. 20, only the fundamental harmonic is observed, both prior to and during the GIC event. As a result, the reactive power consumption remains effectively unchanged throughout the simulation.

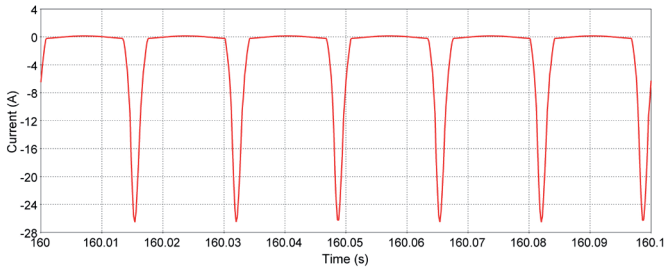

Fig. 16. Magnetizing current of the step-up power transformer in Node 42 during GIC conditions, without the capacitor installed

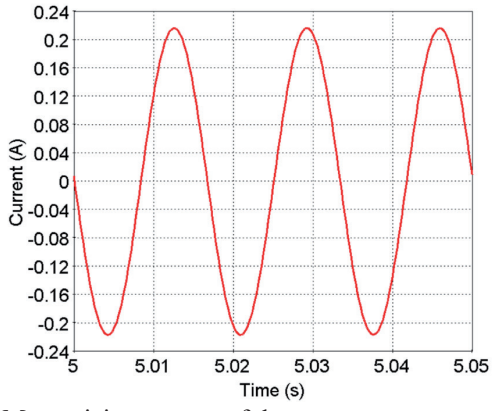

Fig. 17. Magnetizing current of the step-up power transformer in Node 42 with a capacitor installed in the transformer star point before the inclusion of GIC

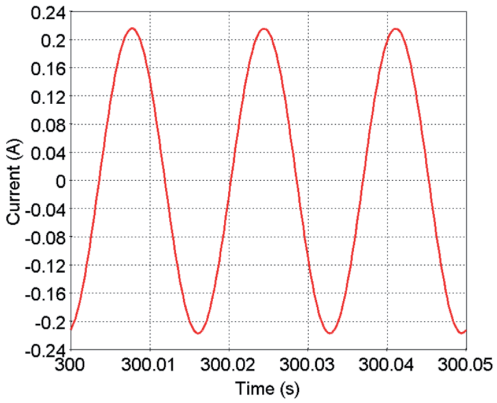

Fig. 18. Magnetizing current of the step-up power transformer in Node 42 with a capacitor installed in the transformer star point during the GIC

Antonio Gloc, Bruno Jurišić, Božidar Filipović-Grčić, Geomagnetically Induced Currents and Influence on Power Transformer Saturation, Journal of Energy, vol. 75 Number 3 (2026), 43–49
https://doi.org/10.37798/2026753768
© 2026 Copyright for this paper by authors. Use permitted under Creative Commons Attribution-NonCommercial (CC BY-NC) 4.0 International License

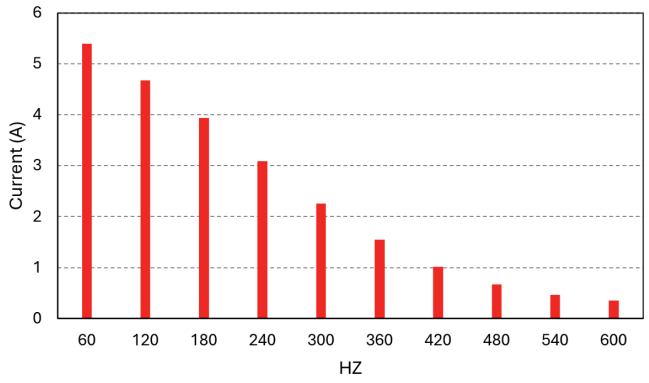

Fig. 19. Harmonic content of the magnetizing current in the step-up power transformer at Node 42 under GIC conditions without capacitor installed

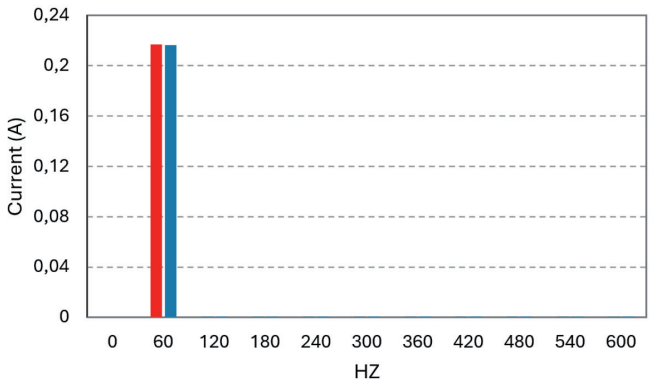

Fig. 20. Harmonic content of the magnetizing current in the step-up power transformer at Node 42 under GIC conditions with capacitor installed (before GIC—red, during GIC—blue)

E. Change in the transformer connection group supplying the loads from Yd to Dy

In the following simulation, node 42 remains under observation, with both the step-up transformer and the load-serving transformer included in the analysis. The load-serving transformer is initially connected in the YNd11 vector group, with a rated voltage of 25/138 kV and a rated power of 125 MVA. Changing its connection group from Yd to Dy alters the path of GIC flow in the bus. The connection group was changed on all transformers supplying the load, the remaining transformers were not modified. Previously, GIC could of flow through the HV windings in a star connection. By changing the connection group to a delta connection, current can no longer close through the HV windings of transformers used to supply the load. As a result, after the connection group change, GIC closes through the star points of the block transformers (which have a Dyn connection group) or through the node containing both the block transformer and the load. For better understanding of the simulation results and the phenomena in the model, Fig. 21 shows the direction of GIC flow within Node 42, to which the block transformer and load are connected.

Once the GIC current enters the node, it can no longer split between the block transformer and the load supplying transformer. After the connection group changes, the current closes only through the block transformer to ground and then returns via the ground to the star point of the transformer supplying the load (on the LV side where the winding is in an yn connection). For this reason, the GIC through the star point of the transformer supplying the load is almost equal in magnitude but opposite in polarity. Small differences in the results are caused by losses in the active and reactive resistance used to model the grounding. Due to this described circulation of GIC current, large changes occur in transformer saturation, higher harmonic generation, reactive power consumption, and other effects.

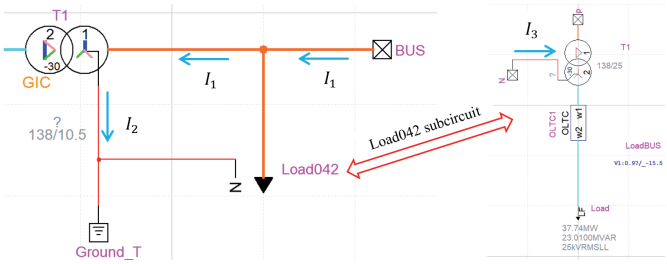

Fig. 21. Flow of GIC within Node 42 after the connection group of the transformer supplying the load was changed

Fig. 22 shows that following a change in the transformer connection group, the GIC through the block transformer flows through its grounding with positive polarity, in other words, it moves toward the ground with a substantially higher amplitude than before. Fig. 23 illustrates the GIC of negative polarity through the star point of the transformer supplying the load, indicating that the GIC enters from the ground side, in this case, a significant increase in amplitude is also observed. Due to this circulation of the GIC, both transformers are subjected to increased stress and are more vulnerable to negative effects.

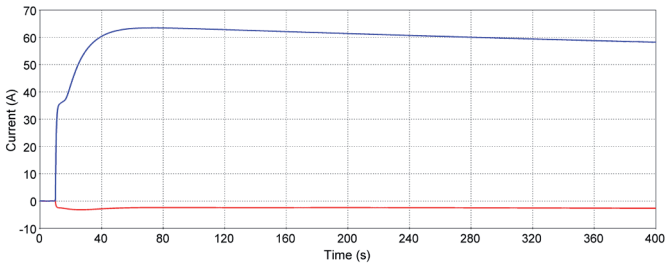

Fig. 22. Current through the grounding of the block transformer in Node 42 (Base case – red curve, after changing the transformer connection group (I_2) – blue curve)

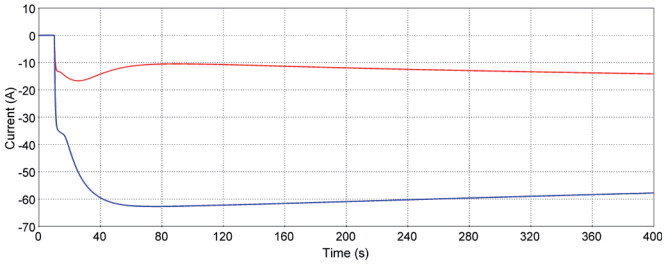

Fig. 23. Current through the grounding of the load-supplying transformer in Node 42 (Base case – red curve, after changing the transformer connection (I_3) – blue curve)

The increase in GIC, as previously described, affects both the magnitude and distortion of the magnetizing current. In the block transformer, the magnetizing current changed completely Fig. 24. Whereas it was previously negative with an amplitude of only 7.2 A, after the change in connection group it became positive and amplitude increased to 128.8 A. In the transformer supplying the load, changes of the same magnitude did not occur, in fact, the amplitude of the magnetizing current decreased while retaining a negative polarity Fig. 25. This can be attributed to the entrance of GIC through the star point into the LV winding of the transformer. The change in the magnetizing current amplitude also affects the harmonic content. Harmonic amplitudes of the current resulting from the transformer connection group change, compared with the base model, for the block transformer Fig. 26, and for the transfor-

Antonio Gloc, Bruno Jurišić, Božidar Filipović-Grčić, Geomagnetically Induced Currents and Influence on Power Transformer Saturation, Journal of Energy, vol. 75 Number 3 (2026), 43–49
https://doi.org/10.37798/2026753768
© 2026 Copyright for this paper by authors. Use permitted under Creative Commons Attribution-NonCommercial (CC BY-NC) 4.0 International License

mer supplying the load Fig. 27.

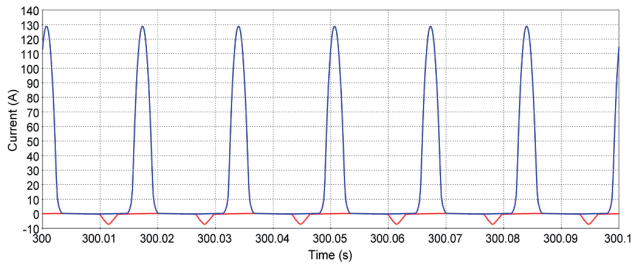

Fig. 24. Change in the magnetizing current of the block transformer core at Node 42 (Base case – red curve, after changing the transformer connection – blue curve)

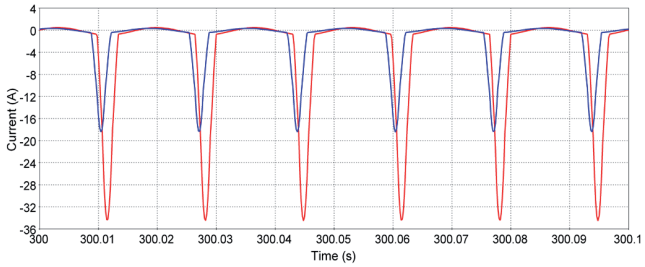

Fig. 25. Change in the magnetizing current of the transformer core supplying the load at Node 42 (Base case – red curve; after transformer connection change – blue curve)

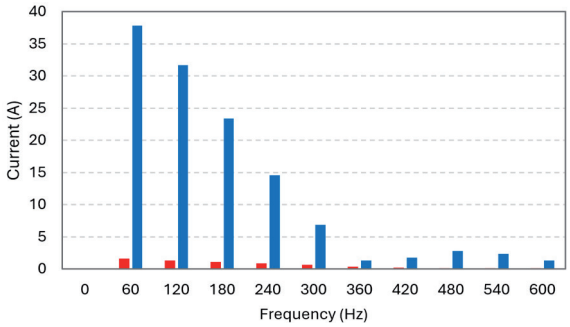

Fig. 26. Harmonics of the magnetizing current of the block transformer core at Node 42 (Base case – red, after changing the transformer connection – blue)

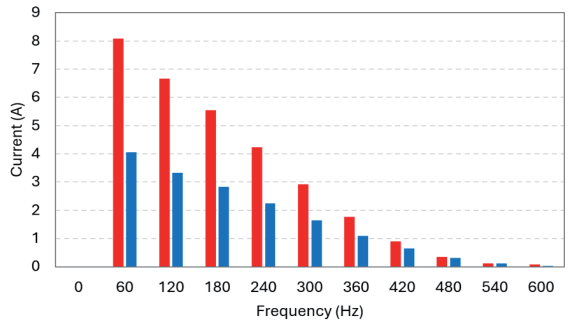

Fig. 27. Harmonics of the magnetizing current of the load-connected transformer at Node 42 (Base case – red, after changing the transformer connection – blue)

V. Conclusion

The impact of geomagnetically induced currents (GIC) depends on numerous factors, including geographic latitude, the intensity of the geomagnetic storm, the direction of geomagnetic field propagation relative to the transmission line, the operating voltage level, the resistance and length of the transmission line, and transformer characteristics such as core type and connection group. The flow of direct current through transformers causes core saturation, which leads to the appearance of higher current and voltage harmonics in the power system, as well as large reactive power consumption and voltage drops in the network. If the lack of reactive power cannot be compensated, the voltage throughout the system drops, which may cause cascading failures of network elements or even lead to a complete system collapse. For a successful analysis of GIC, it is necessary to develop a high voltage, nonlinear power system model that includes detailed models of individual components. This entails modeling the dynamic response of generators, excitation systems, the time dependent behavior of control switches, compensation devices, FACTS systems, power electronics, and other elements present in the network. Such a model was developed in EMTP (Electromagnetic Transients Program) to enable time domain simulations of transient phenomena, where the simulations should be preliminarily supported by an unbalanced three-phase power flow calculation. Only with this approach is it possible to obtain relevant and physically credible results.

Acknowledgment:

The research was funded by the European Union's NextGenerationEU programme, as part of the institutional project "Resilient Self-Healing Future Power Systems – RePowerFER," which is included in the programme agreement of the University of Zagreb Faculty of Electrical Engineering and Computing. The views and opinions expressed are solely those of the author and do not necessarily reflect the official position of the European Union or the European Commission. Neither the European Union nor the European Commission can be held responsible for them.

References

[1] N. Yufan, Development of Magnetic Models to Assess Transformers' Susceptibility to Geomagnetic Disturbances, 2018.

[2] D. Žarko and B. Ćućić, "Transformatori u teoriji i praksi," Graphis, Zagreb, 2021.

[3] D. Žarko and Z. Maljković, Osnove transformatora, Zagreb: Sveučilište u Zagrebu Fakultet elektrotehnike i računarstva, 2016.

[4] WG C4.32, TB 780, "Understanding of geomagnetic storm environment for high voltage power grids," Cigre, 2019.

[5] WG A2.57, TB 944, Effects of DC Bias on power transformers, Cigre, November 2024.

[6] L. Gerin-Lajoie, S. Guillon, J. Mahseredjian and O. Saad, Impact of transformer saturation from GIC on power system voltage regulation, Vancouver, 2013.

[7] L. L. van der Zel, Mitigation od Geomagnetically Induced Currents in Transformers, Electric power reserche institute, 2006.

[8] P. Schachinger, D. Albert and H. Renner, Reduction of geomagnetically induced current impacts by optimized neutral point connections, Graz: The Institute of Engineering and Technology, 2023.

[9] A. Haddadi, A. Rezaei-Zare, R. Hassani, J. Mahseredjian and L. Gerin-Lajoie, A Modified IEEE 118-Bus Test Case for Geomagnetic Disturbance Studies–Part I: Model Data, IEEE, 2020.

[10] A. Haddadi, L. Gerin-Lajoie, A. Rezaei-Zare, R. Hassani and J. Mahseredjian, A Modified IEEE 118-Bus Test Case for Geomagnetic Disturbance Studies—Part II: Simulation Results, IEEE, 2020.

[11] R. Girgis, K. Vedante and K. Gramm, "Effects of Geomagnetically Induced Currents on Power Transformers and Power Systems," Cigre, 2012.

Antonio Gloc, Bruno Jurišić, Božidar Filipović-Grčić, Geomagnetically Induced Currents and Influence on Power Transformer Saturation, Journal of Energy, vol. 75 Number 3 (2026), 43–49
https://doi.org/10.37798/2026753768
© 2026 Copyright for this paper by authors. Use permitted under Creative Commons Attribution-NonCommercial (CC BY-NC) 4.0 International License